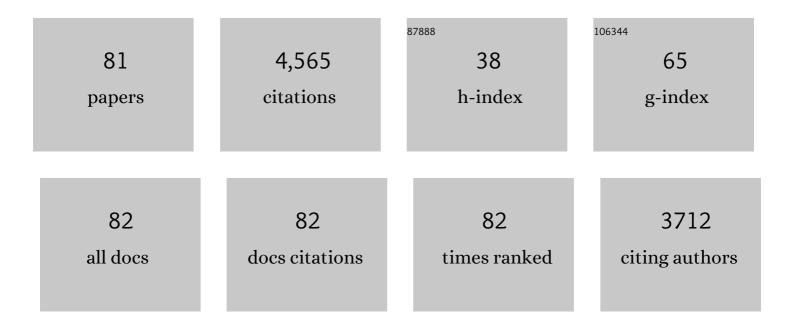
## Minghui Zhu

List of Publications by Year in descending order

Source: https://exaly.com/author-pdf/7944215/publications.pdf Version: 2024-02-01



#	Article	IF	CITATIONS
1	Iron-Based Catalysts for the High-Temperature Water–Gas Shift (HT-WGS) Reaction: A Review. ACS Catalysis, 2016, 6, 722-732.	11.2	267
2	Nature of Active Sites and Surface Intermediates during SCR of NO with NH <sub>3</sub> by Supported V <sub>2</sub> O <sub>5</sub> –WO <sub>3</sub> /TiO <sub>2</sub> Catalysts. Journal of the American Chemical Society, 2017, 139, 15624-15627.	13.7	266
3	Covalently Grafting Cobalt Porphyrin onto Carbon Nanotubes for Efficient CO <sub>2</sub> Electroreduction. Angewandte Chemie - International Edition, 2019, 58, 6595-6599.	13.8	190
4	Reconstructed covalent organic frameworks. Nature, 2022, 604, 72-79.	27.8	190
5	Elucidating the Reactivity and Mechanism of CO <sub>2</sub> Electroreduction at Highly Dispersed Cobalt Phthalocyanine. ACS Energy Letters, 2018, 3, 1381-1386.	17.4	175
6	Essential Role of the Support for Nickel-Based CO <sub>2</sub> Methanation Catalysts. ACS Catalysis, 2020, 10, 14581-14591.	11.2	165
7	Synergistic Effect of Atomically Dispersed Ni–Zn Pair Sites for Enhanced CO <sub>2</sub> Electroreduction. Advanced Materials, 2021, 33, e2102212.	21.0	155
8	Induced activation of the commercial Cu/ZnO/Al2O3 catalyst for the steam reforming of methanol. Nature Catalysis, 2022, 5, 99-108.	34.4	155
9	Unraveling Highly Tunable Selectivity in CO <sub>2</sub> Hydrogenation over Bimetallic In-Zr Oxide Catalysts. ACS Catalysis, 2019, 9, 8785-8797.	11.2	139
10	Influence of catalyst synthesis method on selective catalytic reduction (SCR) of NO by NH3 with V2O5-WO3/TiO2 catalysts. Applied Catalysis B: Environmental, 2016, 193, 141-150.	20.2	136
11	Cobalt phthalocyanine coordinated to pyridine-functionalized carbon nanotubes with enhanced CO2 electroreduction. Applied Catalysis B: Environmental, 2019, 251, 112-118.	20.2	135
12	A decade+ of operando spectroscopy studies. Catalysis Today, 2017, 283, 27-53.	4.4	126
13	Building a stable cationic molecule/electrode interface for highly efficient and durable CO <sub>2</sub> reduction at an industrially relevant current. Energy and Environmental Science, 2021, 14, 483-492.	30.8	101
14	Vacancy engineering of the nickel-based catalysts for enhanced CO2 methanation. Applied Catalysis B: Environmental, 2021, 282, 119561.	20.2	100
15	Promotion Mechanisms of Iron Oxide-Based High Temperature Water–Gas Shift Catalysts by Chromium and Copper. ACS Catalysis, 2016, 6, 4455-4464.	11.2	98
16	Direct Electrochemical Carboxylation of Benzylic C–N Bonds with Carbon Dioxide. ACS Catalysis, 2019, 9, 4699-4705.	11.2	98
17	Strong Metal–Support Interactions between Copper and Iron Oxide during the Highâ€īemperature Waterâ€Gas Shift Reaction. Angewandte Chemie - International Edition, 2019, 58, 9083-9087.	13.8	82
18	Reaction Pathways and Kinetics for Selective Catalytic Reduction (SCR) of Acidic NO <sub><i>x</i></sub> Emissions from Power Plants with NH <sub>3</sub> . ACS Catalysis, 2017, 7, 8358-8361.	11.2	78

Мілсниі Zhu

#	Article	IF	CITATIONS
19	Formation of N2O greenhouse gas during SCR of NO with NH3 by supported vanadium oxide catalysts. Applied Catalysis B: Environmental, 2018, 224, 836-840.	20.2	72
20	Unraveling the Role of Zinc on Bimetallic Fe <sub>5</sub> C <sub>2</sub> –ZnO Catalysts for Highly Selective Carbon Dioxide Hydrogenation to High Carbon α-Olefins. ACS Catalysis, 2021, 11, 2121-2133.	11.2	72
21	Dynamics of CrO <sub>3</sub> –Fe <sub>2</sub> O <sub>3</sub> Catalysts during the High-Temperature Water-Gas Shift Reaction: Molecular Structures and Reactivity. ACS Catalysis, 2016, 6, 4786-4798.	11.2	68
22	Structural Buffer Engineering on Metal Oxide for Longâ€Term Stable Seawater Splitting. Advanced Functional Materials, 2022, 32, .	14.9	64
23	Ni-based catalysts derived from Ni-Zr-Al ternary hydrotalcites show outstanding catalytic properties for low-temperature CO2 methanation. Applied Catalysis B: Environmental, 2021, 293, 120218.	20.2	62
24	The study of structure-performance relationship of iron catalyst during a full life cycle for CO2 hydrogenation. Journal of Catalysis, 2019, 378, 51-62.	6.2	60
25	Elucidation of the Reaction Mechanism for High-Temperature Water Gas Shift over an Industrial-Type Copper–Chromium–Iron Oxide Catalyst. Journal of the American Chemical Society, 2019, 141, 7990-7999.	13.7	60
26	Inductive and electrostatic effects on cobalt porphyrins for heterogeneous electrocatalytic carbon dioxide reduction. Catalysis Science and Technology, 2019, 9, 974-980.	4.1	56
27	Structureâ€Tunable Copper–Indium Catalysts for Highly Selective CO <sub>2</sub> Electroreduction to CO or HCOOH. ChemSusChem, 2019, 12, 3955-3959.	6.8	55
28	Probing the role of surface hydroxyls for Bi, Sn and In catalysts during CO2 Reduction. Applied Catalysis B: Environmental, 2021, 298, 120581.	20.2	54
29	Selective catalytic reduction of NO by NH3 with WO3-TiO2 catalysts: Influence of catalyst synthesis method. Applied Catalysis B: Environmental, 2016, 188, 123-133.	20.2	51
30	Selective methane electrosynthesis enabled by a hydrophobic carbon coated copper core–shell architecture. Energy and Environmental Science, 2022, 15, 234-243.	30.8	51
31	Recent Advances in Electrochemical CO <sub>2</sub> Reduction on Indiumâ€Based Catalysts. ChemCatChem, 2021, 13, 514-531.	3.7	50
32	Tracking structural evolution: <i>operando</i> regenerative CeOx/Bi interface structure for high-performance CO2 electroreduction. National Science Review, 2021, 8, nwaa187.	9.5	50
33	Resolving the Reaction Mechanism for H <sub>2</sub> Formation from High-Temperature Water–Gas Shift by Chromium–Iron Oxide Catalysts. ACS Catalysis, 2016, 6, 2827-2830.	11.2	48
34	Structure–Activity Relationships of Copper- and Potassium-Modified Iron Oxide Catalysts during Reverse Water–Gas Shift Reaction. ACS Catalysis, 2021, 11, 12609-12619.	11.2	48
35	Nature of Reactive Oxygen Intermediates on Copper-Promoted Iron–Chromium Oxide Catalysts during CO <sub>2</sub> Activation. ACS Catalysis, 2020, 10, 7857-7863.	11.2	44
36	Uncovering the electronic effects of zinc on the structure of Fe5C2-ZnO catalysts for CO2 hydrogenation to linear α-olefins. Applied Catalysis B: Environmental, 2021, 295, 120287.	20.2	44

Мілсниі Zhu

#	Article	IF	CITATIONS
37	Operando Highâ€Valence Crâ€Modified NiFe Hydroxides for Water Oxidation. Small, 2022, 18, e2200303.	10.0	44
38	Tuning the Metal Electronic Structure of Anchored Cobalt Phthalocyanine via Dualâ€Regulator for Efficient CO <sub>2</sub> Electroreduction and Zn–CO <sub>2</sub> Batteries. Advanced Functional Materials, 2022, 32, .	14.9	43
39	Resolving CO2 activation and hydrogenation pathways over iron carbides from DFT investigation. Journal of CO2 Utilization, 2020, 38, 10-15.	6.8	41
40	Determining Number of Active Sites and TOF for the High-Temperature Water Gas Shift Reaction by Iron Oxide-Based Catalysts. ACS Catalysis, 2016, 6, 1764-1767.	11.2	36
41	Strong Metal–Support Interactions between Nickel and Iron Oxide during CO <sub>2</sub> Hydrogenation. ACS Catalysis, 2021, 11, 11966-11972.	11.2	36
42	Promotional effect of Mn-doping on the structure and performance of spinel ferrite microspheres for CO hydrogenation. Journal of Catalysis, 2020, 381, 150-162.	6.2	35
43	Chemical and structural properties of Na decorated Fe5C2-ZnO catalysts during hydrogenation of CO2 to linear α-olefins. Applied Catalysis B: Environmental, 2021, 298, 120567.	20.2	35
44	Electronic Tuning of Cobalt Porphyrins Immobilized on Nitrogen-Doped Graphene for CO <sub>2</sub> Reduction. ACS Applied Energy Materials, 2019, 2, 2435-2440.	5.1	34
45	Facile synthesis of polymerized cobalt phthalocyanines for highly efficient CO <sub>2</sub> reduction. Green Chemistry, 2019, 21, 6056-6061.	9.0	33
46	Superfast and Waterâ€Insensitive Polymerization on αâ€Amino Acid <i>N</i> â€Carboxyanhydrides to Prepare Polypeptides Using Tetraalkylammonium Carboxylate as the Initiator. Angewandte Chemie - International Edition, 2021, 60, 26063-26071.	13.8	33
47	Dynamic structure of highly disordered manganese oxide catalysts for low-temperature CO oxidation. Journal of Catalysis, 2021, 401, 115-128.	6.2	31
48	Highly Active and Selective Multicomponent Fe–Cu/CeO <sub>2</sub> –Al <sub>2</sub> O <sub>3</sub> Catalysts for CO <sub>2</sub> Upgrading via RWGS: Impact of Fe/Cu Ratio. ACS Sustainable Chemistry and Engineering, 2021, 9, 12155-12166.	6.7	30
49	Revealing structure-activity relationships in chromium free high temperature shift catalysts promoted by earth abundant elements. Applied Catalysis B: Environmental, 2018, 232, 205-212.	20.2	27
50	Formation and influence of surface hydroxyls on product selectivity during CO2 hydrogenation by Ni/SiO2 catalysts. Journal of Catalysis, 2021, 400, 228-233.	6.2	27
51	Effect of MnO <sub>2</sub> Polymorphs' Structure on Low-Temperature Catalytic Oxidation: Crystalline Controlled Oxygen Vacancy Formation. ACS Applied Materials & Interfaces, 2022, 14, 18525-18538.	8.0	27
52	Covalently Grafting Cobalt Porphyrin onto Carbon Nanotubes for Efficient CO <sub>2</sub> Electroreduction. Angewandte Chemie, 2019, 131, 6667-6671.	2.0	26
53	Syngas production and trace element emissions from microwave-assisted chemical looping gasification of heavy metal hyperaccumulators. Science of the Total Environment, 2019, 659, 612-620.	8.0	25
54	In Operando Identification of In Situ Formed Metalloid Zinc <sup>δ+</sup> Active Sites for Highly Efficient Electrocatalyzed Carbon Dioxide Reduction. Angewandte Chemie - International Edition, 2022, 61, .	13.8	25

Мілсниі Zhu

#	Article	IF	CITATIONS
55	Probing the surface of promoted CuO-Cr2O3-Fe2O3 catalysts during CO2 activation. Applied Catalysis B: Environmental, 2020, 271, 118943.	20.2	24
56	Fundamental nanoscale surface strategies for robustly controlling heterogeneous nucleation of calcium carbonate. Journal of Materials Chemistry A, 2019, 7, 17242-17247.	10.3	23
57	A perspective on chromium-Free iron oxide-based catalysts for high temperature water-gas shift reaction. Catalysis Today, 2018, 311, 2-7.	4.4	22
58	Strong Metal–Support Interactions between Copper and Iron Oxide during the Highâ€Temperature Waterâ€Gas Shift Reaction. Angewandte Chemie, 2019, 131, 9181-9185.	2.0	22
59	Revealing the Effect of Sodium on Iron-Based Catalysts for CO <sub>2</sub> Hydrogenation: Insights from Calculation and Experiment. Journal of Physical Chemistry C, 2021, 125, 7637-7646.	3.1	20
60	Ternary Fe–Zn–Al Spinel Catalyst for CO <sub>2</sub> Hydrogenation to Linear α-Olefins: Synergy Effects between Al and Zn. ACS Sustainable Chemistry and Engineering, 2021, 9, 13818-13830.	6.7	20
61	Molecular structure and sour gas surface chemistry of supported K2O/WO3/Al2O3 catalysts. Applied Catalysis B: Environmental, 2018, 232, 146-154.	20.2	19
62	Tunable Carbon Dioxide Activation Pathway over Iron Oxide Catalysts: Effects of Potassium. Industrial & Engineering Chemistry Research, 2021, 60, 8705-8713.	3.7	18
63	Nature and Reactivity of Oxygen Species on/in Silver Catalysts during Ethylene Oxidation. ACS Catalysis, 2022, 12, 4375-4381.	11.2	17
64	Structure–Activity Relationship of the Polymerized Cobalt Phthalocyanines for Electrocatalytic Carbon Dioxide Reduction. Journal of Physical Chemistry C, 2020, 124, 16501-16507.	3.1	16
65	Activation and deactivation of the commercialâ€ŧype CuO–Cr <sub>2</sub> O <sub>3</sub> –Fe <sub>2</sub> O <sub>3</sub> high temperature shift catalyst. AICHE Journal, 2020, 66, e16846.	3.6	14
66	Pyridine-grafted nitrogen-doped carbon nanotubes achieving efficient electroreduction of CO <sub>2</sub> to CO within a wide electrochemical window. Journal of Materials Chemistry A, 2022, 10, 1852-1860.	10.3	12
67	Curvature-induced electronic tuning of molecular catalysts for CO <sub>2</sub> reduction. Catalysis Science and Technology, 2021, 11, 2491-2496.	4.1	11
68	Revealing the dependence of CO <sub>2</sub> activation on hydrogen dissociation ability over supported nickel catalysts. AICHE Journal, 2022, 68, e17458.	3.6	9
69	Controlling the Reconstruction of Ni/CeO2 Catalyst during Reduction for Enhanced CO Methanation. Engineering, 2022, 14, 94-99.	6.7	9
70	Synthesis, size reduction, and delithiation of carbonate-free nanocrystalline lithium nickel oxide. Journal of Materials Science, 2013, 48, 1740-1745.	3.7	8
71	Phthalocyanine-derived catalysts decorated by metallic nanoclusters for enhanced CO2 electroreduction. Green Energy and Environment, 2023, 8, 444-451.	8.7	7
72	Combined <i>In Situ</i> Diffuse Reflectance Infrared Fourier Transform Spectroscopy and Kinetic Studies on CO <sub>2</sub> Methanation Reaction over Ni/Al <sub>2</sub> O <sub>3</sub> . Industrial & Engineering Chemistry Research, 2022, 61, 9678-9685.	3.7	7

Мімсниї Zhu

#	Article	IF	CITATIONS
73	Superfast and Waterâ€Insensitive Polymerization on αâ€Amino Acid <i>N</i> â€Carboxyanhydrides to Prepare Polypeptides Using Tetraalkylammonium Carboxylate as the Initiator. Angewandte Chemie, 2021, 133, 26267-26275.	2.0	5
74	Electrochemical conversion of CO <sub>2</sub> to syngas with a stable H <sub>2</sub> /CO ratio in a wide potential range over ligand-engineered metal–organic frameworks. Journal of Materials Chemistry A, 2022, 10, 9954-9959.	10.3	5
75	Syngas to olefins with low CO2 formation by tuning the structure of FeCx-MgO-Al2O3 catalysts. Chemical Engineering Journal, 2022, 450, 137167.	12.7	5
76	A Review on the Waterâ€Gas Shift Reaction over Nickelâ€Based Catalysts. ChemCatChem, 2022, 14, .	3.7	5
77	Elucidating the reactivity and nature of active sites for tin phthalocyanine during CO <sub>2</sub> reduction. , 2021, 11, 1191-1197.		4
78	Unravelling the metal–support interactions in χ-Fe <sub>5</sub> C <sub>2</sub> /MgO catalysts for olefin synthesis directly from syngas. Catalysis Science and Technology, 2022, 12, 762-772.	4.1	4
79	Electroreduction of Carbon Dioxide by Heterogenized Cofacial Porphyrins. Transactions of Tianjin University, 0, , 1.	6.4	3
80	Effect of micropores on the structure and CO <sub>2</sub> methanation performance of supported Ni/SiO <sub>2</sub> catalyst. , 2021, 11, 1213-1221.		3
81	Operando Metalloid Znδ+ Active Sites for Highly Efficient Carbon Dioxide Reduction Electrocatalysis. Angewandte Chemie, 0, , .	2.0	0